Brazilian Journal of Geophysics
Brazilian Geophysical Society
ISSN 2764-8044
DOI: 10.22564/brjg.v43i3.2345

INTEGRATION OF GRAVITY DISTURBANCE AND BOUGUER DISTURBANCE FOR GEOLOGICAL AND GEOPHYSICAL MAPPING IN PARANÁ STATE, SOUTHERN BRAZIL

Eros Kerouak Cordeiro Pereira[1], Alessandra de Barros e Silva Bongiolo[1], Luizemara Soares Alves Szameitat[2], Tiago Lima Rodrigues[1], and Francisco José Fonseca Ferreira[1]

[1]Universidade Federal do Paraná - UFPR, Curitiba, PR, Brazil
[2]Observatório Nacional - ON, Rio de Janeiro, RJ, Brazil

Pereira: https://orcid.org/0009-0008-0891-6781
Bongiolo: https://orcid.org/0000-0001-7142-0043
Szameitat: https://orcid.org/0000-0002-1148-5635
Rodrigues: https://orcid.org/0000-0002-3037-9037
Ferreira: https://orcid.org/0000-0002-0269-5833

Corresponding author e-mail: eroskerouak@gmail.com

ABSTRACT. This article presents a gravity data integration and a regional geophysical overview of the geological framework in the State of Paraná, southern Brazil. For data processing, we used open-source computational tools based on Python libraries from the Fatiando a Terra Project. Data processing included determining theoretical gravity on the physical surface of the Earth, calculating the Gravity Disturbance, modeling topographic masses to obtain the complete Bouguer Disturbance, data gridding using the equivalent source method, and the application of enhancement techniques. The products obtained were compared with previous geological studies, revealing a robust correlation between our results and the main geological characteristics from literature. Some relatively high values of the Bouguer Disturbance indicate important structural features, such as the Paranapanema Block and the Ponta Grossa Arch. Additionally, enhancement techniques highlighted relevant geological structures, in both the Paraná Basin and the Proterozoic orogenic basement. Using the gravity method and open-source tools, this work aims to serve as a reference for future geophysical and geological investigations in the State of Paraná. The gravity maps of the Paraná are a valuable unified database for the scientific community and for future geophysical investigations. These data will be made available in an open repository, facilitating access and encouraging use in subsequent research and practical applications.

Keywords: Gravity Database; Bouguer Disturbance; Paranapanema Block; Paraná Basin; Ponta Grossa Arch

INTRODUCTION

In this work, various available gravimetric data were integrated, revealing the main first-order structures of the geological framework of the State of Paraná, southern Brazil. The focus was on the integration and analysis of the available gravimetric data, using internally developed Python codes based on libraries and techniques published by the Fatiando a Terra Project (Uieda et al., 2013). These algorithms are available on the GitHub repository (https://github.com/ErosKerouak/GRAV_PR).

Initially, the Gravity Disturbance was used as the raw gravimetric anomaly instead of the classic Free-Air Anomaly. The chosen gravimetric anomaly benefits from using ellipsoidal heights derived from GNSS records. This method avoids using orthometric heights, which are influenced by the selected geoid model (Segawa, 1984). The Bouguer correction, traditionally applied to free-air anomalies, was then applied to the Gravity

Disturbance, resulting in the so-called Bouguer Disturbance. As defined by Segawa (1984), this is an adaptation of the traditional concept of Bouguer anomaly for Gravity Disturbances instead of free-air anomalies, providing a more accurate reading of the gravitational field, less affected by geoid undulations and more directly related to subsurface density variations. Consequently, the Bouguer Disturbance proves to be particularly effective for geophysical and geological studies aimed at understanding the Earth's crust and upper mantle structure (Segawa, 1984).

A second optimized technique was applied to the interpolation of the data. The equivalent source method (Dampney, 1969; Cooper, 2000; Soler and Uieda, 2021) was employed before applying enhancement filters, such as the Total Horizontal Derivative (THDR), Cordell and Grauch (1985) and the Tilt Derivative (TDR), Miller and Singh (1994).

Finally, to demonstrate the improvement in the compilation of ground gravimetric data in the State of Paraná and the implementation of the new interpolation and processing techniques, the maps from this work were compared with those from Zanon dos Santos et al. (2022).

The objective of this work was to integrate the available ground gravimetric data from various public, private, and academic platforms to obtain an integrated and optimized view of the gravitational features in Paraná, improving the relationship among different sources by constructing a single homogenized database, made publicly available in a repository for future use by the scientific community and industry and serve as a reference for future geophysical and geological investigations in the State of Paraná. To achieve this, ground gravimetric data from different sources were compiled, and Modern techniques for analyzing gravimetric data were adopted.

GEOLOGICAL CONTEXT

The oldest geological records in the State of Paraná are magmatic and metamorphic Proterozoic units, as part of the southeastern continental margin of the South American Plate. In the Phanerozoic Eon, the Proterozoic basement was partially covered by sedimentary units and intruded by magmatic rocks. The simplified geological map of the State of Paraná is shown in Figure 1, where the outcropping basement is represented by NE-oriented units near to the coastline, eastwards. The central and western basement of the State of Paraná is overlaid by sedimentary and volcanic units of Paraná and Bauru basins (Milani et al., 2007).

The Paraná Shield is part of the Ribeira Orogenic System, known as the Southern Ribeira Belt, formed during the agglutination of Western Gondwana (Heilbron et al., 2008). This unit comprises four tectonic compartments: the Apiai, Curitiba, Luis Alves, and Paranagua terranes (Siga Júnior, 1995; Heilbron et al., 2008).

The Paraná Basin is an intracratonic basin (de Almeida et al., 1981) that spans the Second and Third Paranaense Plateaus, covering most of the State of Paraná and extending into other regions of Brazil, Paraguay, Argentina, and Uruguay. It has been filled with sediments across various geological periods, mainly from the Ordovician to the Cretaceous, including siliciclastic sediments, carbonates, and igneous rocks (Milani et al., 2007).

The basin's evolution involved multiple stages of erosion and deposition, separated by regional unconformities. The stratigraphy of the basin is marked by six supersequences: Rio Ivaí (Ordovician-Silurian), Paraná

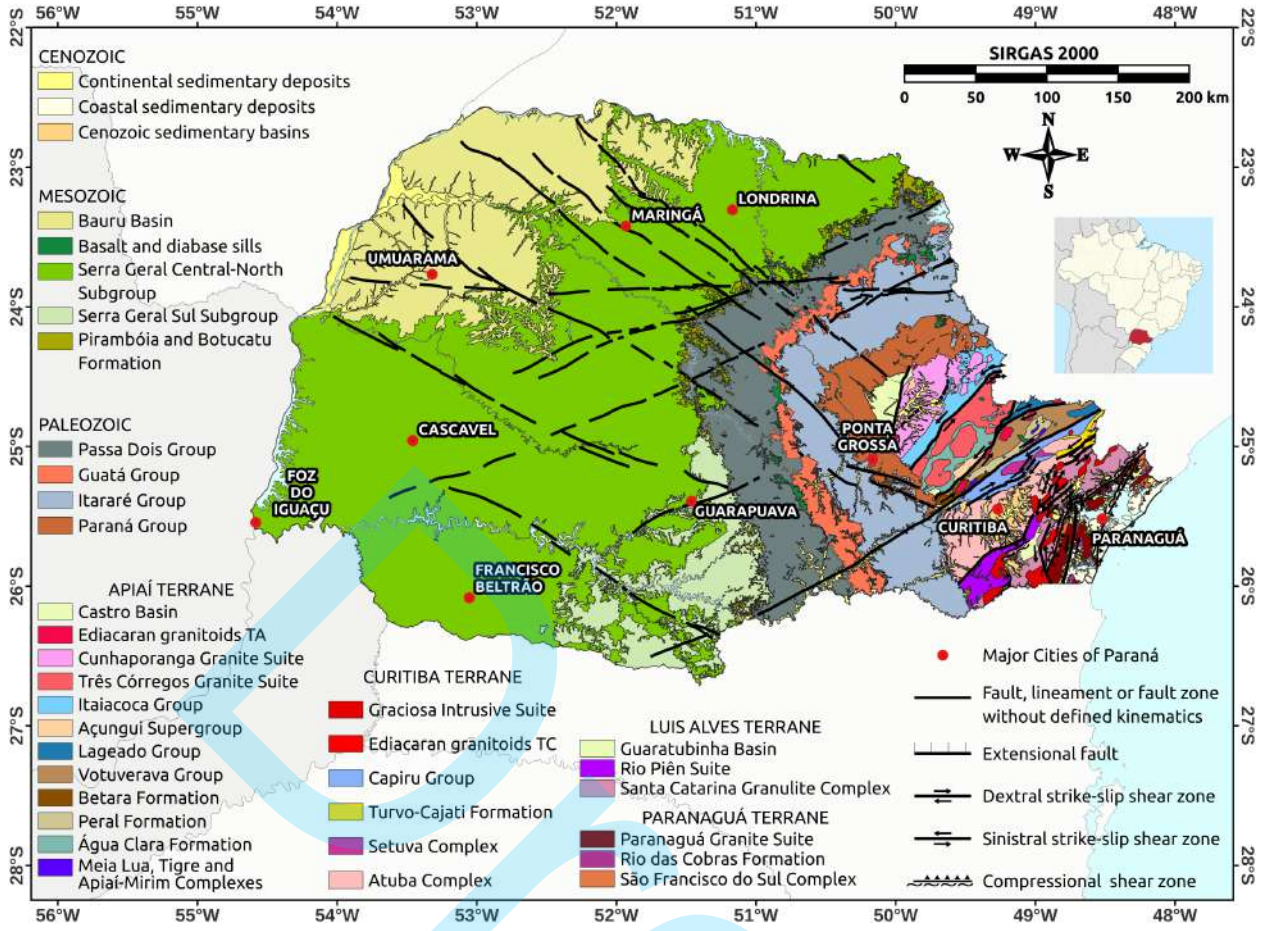

Figure 1: Simplified Geological Map of the State of Paraná, adapted from Besser et al. (2021)

(Devonian), Gondwana I (Carboniferous-Early Triassic), Gondwana II (Mid to Late Triassic), Gondwana III (Late Jurassic-Early Cretaceous), and Bauru (Late Cretaceous) (Milani et al., 2007). Deposited during the Late Cretaceous, the Bauru supersequence marks the final stage of sedimentary infill of the Paraná Basin, manifesting as a set of siliciclastic rocks accumulated in the so-called Bauru Basin (Milani et al., 2007).

In the context of structural geology, Figure 2 presents the main structural lineaments of the State of Paraná, highlighting shear zones, extensional faults, and structures with undefined kinematics. Notable features include the Ponta Grossa Arch, the Ponta Grossa Dike Swarm , and the Paranapanema Block.

The Ponta Grossa Arch is an elevated structure that extends northwestward, with associated structural lineaments and swarms of Early Cretaceous diabase dikes. It is characterized as a broad elevated structure stretching northwest from the coast to the Paraná Basin. This structural formation is notable for the presence of five structural-magnetic lineaments, each with surface extensions of at least 600 km, and associated anomalies covering zones with thicknesses ranging from 20 to 100 km (Portela Filho and Ferreira, 2003).

These lineaments host dense clusters of Early Cretaceous diabase dikes (Renne et al., 1992; Turner et al., 1994). The Ponta Grossa dike swarm shows a subtle displacement toward the southwestern flank of the Ponta Grossa Arch (de Souza Filho and Szameitat, 2022).

The Ponta Grossa Arch represents a crustal uplift and thinning, extending from the coast to the edge of the Paraná Basin. Conversely, the Ponta Grossa Dike Swarm is a narrow linear belt that crosses the Paraná Basin, stretching from the coast nearly to the Brazil-Paraguay border (de Souza Filho and Szameitat, 2022).

Gravimetric studies have defined the existence of a distinct continental block, called the Paranapanema Block, considered a cratonic block located beneath the Paraná Basin. It is characterized by high density and gravitational anomalies, possibly due to mantle refertilization (Mantovani et al., 2005; Chaves et al., 2016).

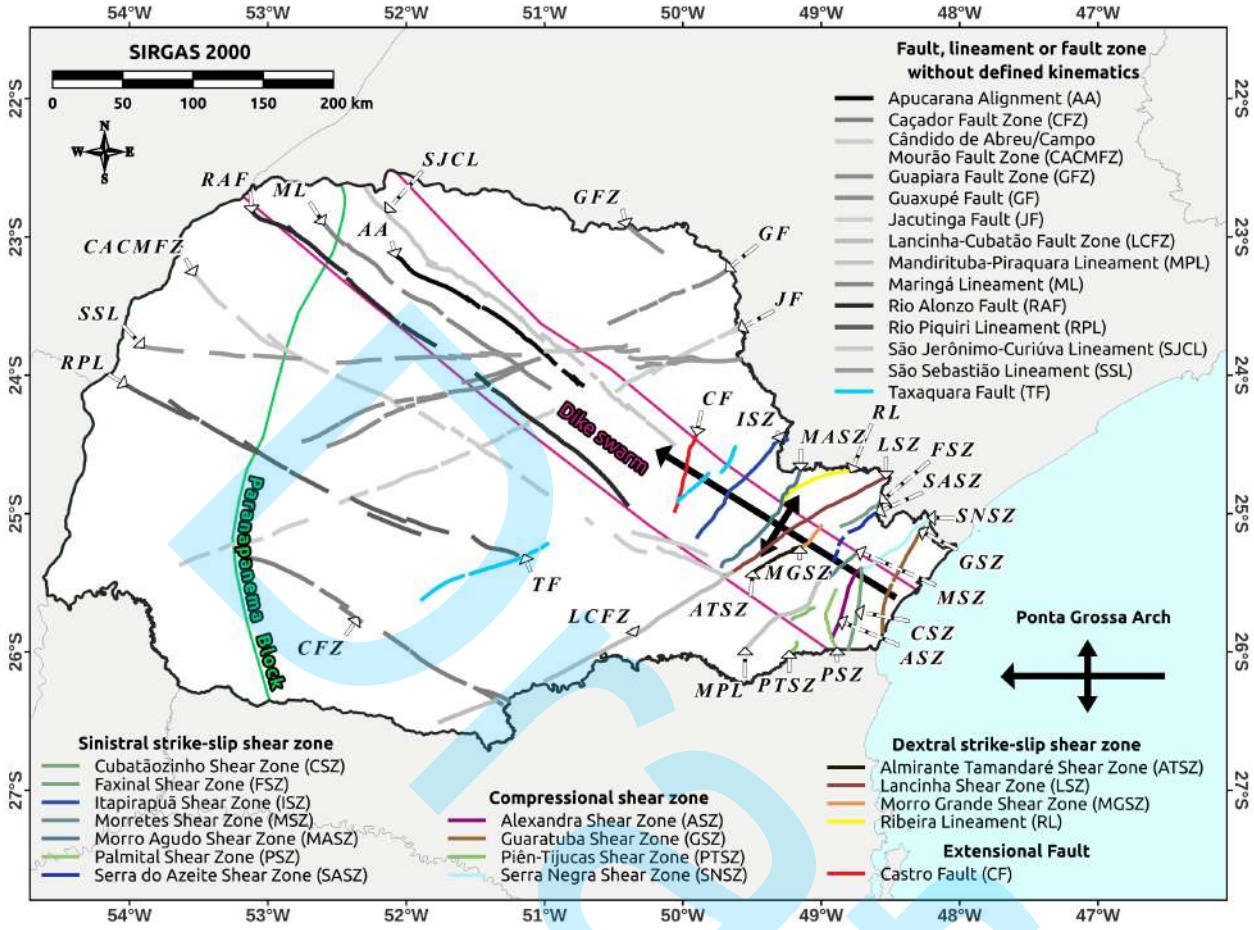

Figure 2: Main Geological Structures in the State of Paraná, adapted from Besser et al. (2021)

MATERIALS AND METHOD

Gravity Data

The data used in this study (Figure 3) were collected by a wide range of institutions, namely Petróleo Brasileiro S/A (Petrobras), Agência Nacional do Petróleo, Gás Natural e Biocombustíveis (National Agency of Petroleum, Natural Gas and Biofuels, ANP), Instituto de Astronomia, Geofísica e Ciências Atmosféricas da Universidade de São Paulo (Institute of Astronomy, Geophysics and Atmospheric Sciences of the University of São Paulo, IAG USP), Instituto Brasileiro de Geografia e Estatística (Brazilian Institute of Geography and Statistics, IBGE), Observatório Nacional (National Observatory, ON), Serviço Geológico do Brasil (Geological Survey of Brazil, SGB/CPRM), and Universidade Federal do Paraná (Federal University of Paraná, UFPR). Figure 3 shows not only the spatial distribution of the ground gravity data, but also the quantitative contribution of each institution to the dataset, expressed as the number of data points provided. Most of this data was included in the compilation of the Banco Nacional de Dados Gravimétricos (National Gravimetric Data Bank, BNDG). It is noteworthy that many of these data are referenced to the Rede Gravimétrica Fundamental Brasileira (Brazilian

Fundamental Gravimetric Network, RGFB), whose administration is carried out by the Observatório Nacional, with the gravimetric datum being International Gravity Standardization Net 1971 (IGSN-71), (Subiza Piña and Sousa, 2001; Luz, 2008).

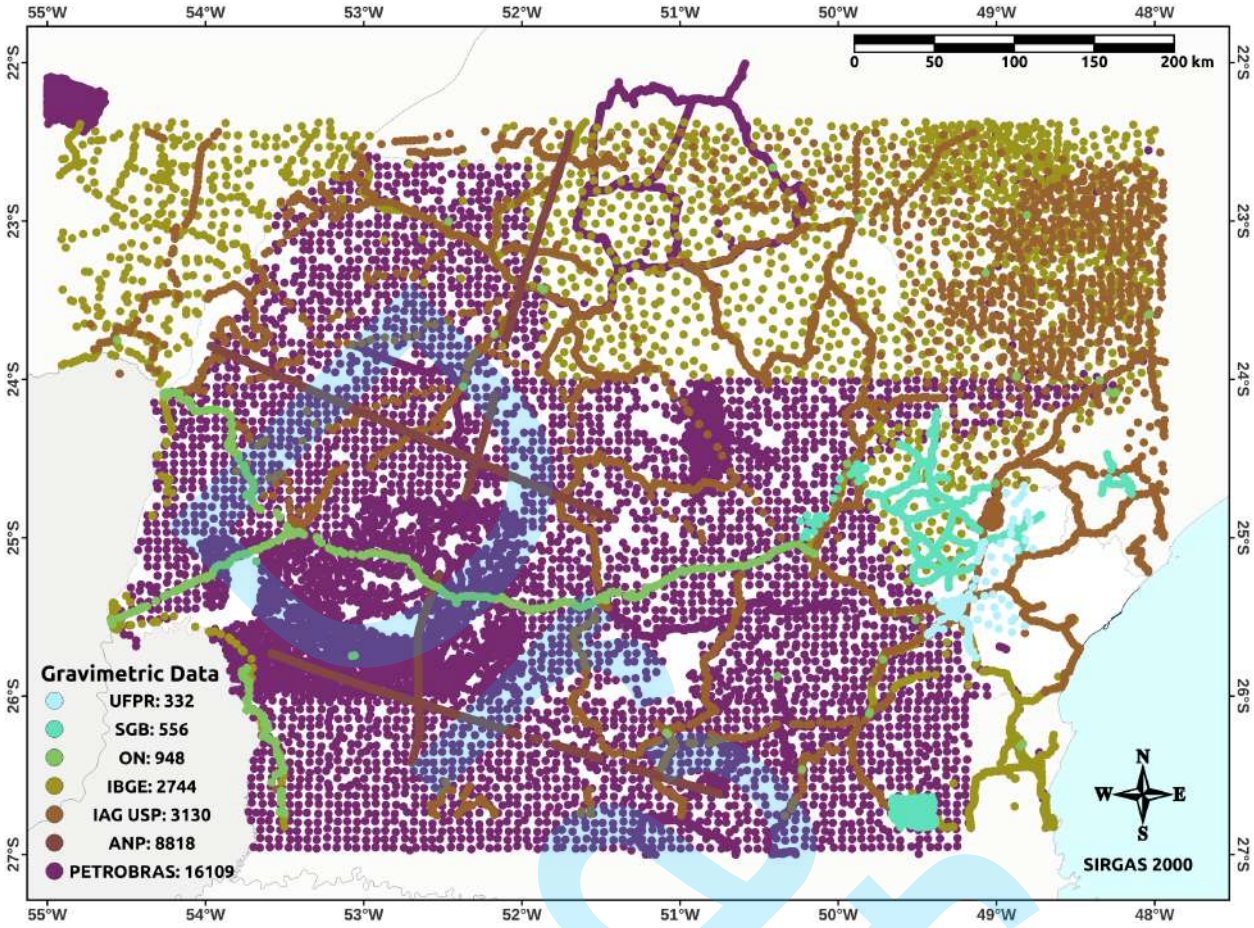

Figure 3: Ground Gravity data in State of Paraná and Surroundings. The spatial distribution and quantitative contribution of each institution, expressed as the number of gravity data points provided, are shown.

Obtaining the Gravity Disturbance

Considering P and Q as points located respectively on the surfaces of the geoid and the ellipsoid, a gravity anomaly Δg is defined as the difference between the magnitude of the actual gravity vector on the geoid surface, g_P, and the magnitude of the theoretical gravity vector on the ellipsoid surface, γ_Q, as follows (Hofmann-Wellenhof and Moritz, 2006):

$$\Delta g = g_P - \gamma_Q. \tag{1}$$

A comparison can be made between the magnitudes of g_P and γ_P, that is, between the magnitude of the actual gravity vector and the magnitude of the theoretical gravity vector, both at the same point P. This comparison results in the calculation of the Gravity Disturbance, δg, expressed by the Equation (Hofmann-Wellenhof and Moritz, 2006):

$$\delta g = g_P - \gamma_P. \tag{2}$$

In this study, the theoretical gravity was obtained using the Boule library (Fatiando a Terra Project et al., 2022), which employs the Lakshmanan and Li-Götze Formula (Lakshmanan, 1991; Götze and Li, 1996; Li and Götze, 2001). Since this formula calculates the theoretical gravity at any height h relative to the ellipsoid, the theoretical gravity value γ_h was directly compared with the observed gravity g_{obs}, yielding the Gravity Disturbance δg as per Equation 2.

The Boule library offers various reference ellipsoids; therefore, the GRS80 ellipsoid was adopted due to its compatibility with GNSS data, which include latitude, longitude, and ellipsoidal height, associated with the gravimetric data. Furthermore, GRS80 is currently the ellipsoid recommended by the International Association of Geodesy (Moritz, 1980).

Obtaining the Bouguer Disturbance

The magnitude of the actual gravity vector on the geoid is estimated using methods such as free-air correction, Bouguer correction, and Helmert condensation, resulting in the so-called free-air and Bouguer anomalies, among others (Heiskanen and Moritz, 1967). Although these tools and concepts are shared by two branches of geoscience, geodesy and geophysics, their application differs due to distinct objectives. In geodesy, for instance, gravity is used to define quasi-geoid models that serve as a reference for height measurements and Earth mapping. In geophysics, gravity assists in the identification of geological features through variations in subsurface density (Li and Götze, 2001).

For geodesy, the Gravity Disturbance on the Earth's surface δg, obtained by Equation 2, eliminates the need for additional reductions. On the other hand, in geophysics, applying the Bouguer reduction to the Gravity Disturbance results in the Bouguer Disturbance, adapting the traditional concept of Bouguer Anomaly to Gravity Disturbances instead of free-air anomalies, a method established by Segawa (1984). The introduction of the Bouguer Disturbance provides a more precise geophysical measurement, less affected by the undulations of the geoid and, consequently, more directly related to subsurface density variations, making it particularly useful for geophysical and geological studies aimed at understanding the structure of the Earth's crust and upper mantle (Segawa, 1984). Additionally, the direct use of ellipsoidal heights, which are now more accurate than orthometric heights and directly obtained via GNSS positioning.

The Bouguer Reduction could be performed in two stages: the effect of the Bouguer Plate and the topographic correction. However, it is also possible to calculate the total effect of the topographic masses in a unified procedure. For this purpose, the masses are modeled using rectangular prisms (Figure 4), allowing the gravitational effect of each prism C_P to be determined at each observation point (Hofmann-Wellenhof and Moritz, 2006).

$$\begin{aligned} \delta g_B &= g_{obs} - \gamma_h - C_P \\ &= \delta g - C_P. \end{aligned} \tag{3}$$

By comparing the measured values with the predicted values for the same points, the Bouguer Disturbance reveals anomalous masses whose densities exceed or are less than a theoretical average value, ρ. The value of 2670 kg/m^3, proposed by Harkness (1891) based on crystalline rocks, is commonly adopted (Hinze, 2003). However, this assumption often does not accurately reflect reality, as demonstrated for the Brazilian territory by de Medeiros et al. (2021).

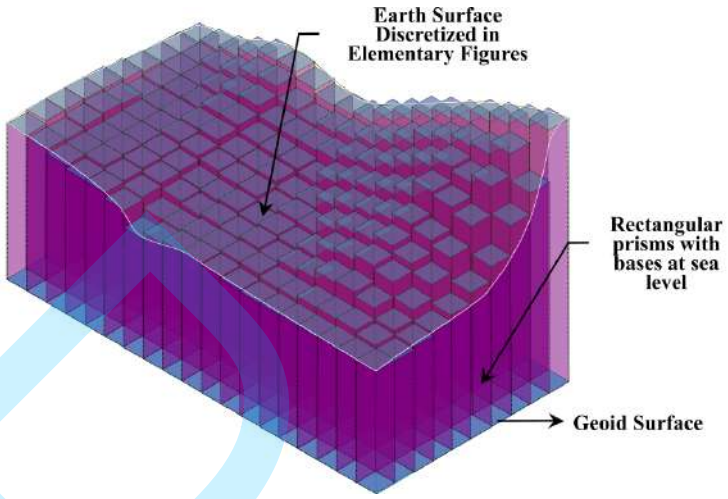

Figure 4: Schematic representation of the Earth surface discretized in elementary figures, where the columns represent rectangular prisms with bases at the sea level.

For this study, the calculation of the complete Bouguer Disturbance was conducted using the Harmonica library (Fatiando a Terra Project et al., 2023). The method employed is based on the direct modeling of topographic masses. The prism_layer algorithm generates a regular grid of prisms with uniform sizes in the horizontal directions, allowing for the adjustment of the upper and lower bounds of each prism. After creating the prisms, the harmonica.prism_gravity function can be used to calculate their gravitational effects at each observation point.

Topographic data from the global digital elevation model FABDEM (Hawker et al., 2022), integrated with bathymetry from SRTM15+ (Tozer et al., 2019), were used in the modeling of prisms, Figure 5a. FABDEM was chosen because it is closer to a digital terrain model as it has undergone filtering of trees and buildings. Given the vast extent of the study area, the topographic data were resampled to a resolution of 500 meters. The density assigned to the prisms was defined based on the Lateral Topographic Density model for Brazil (LTD_Brazil) (de Medeiros et al., 2021), by taking the arithmetic average of the model values for Paraná $\rho = 2512\ kg/m^3$, Figure 5b. Finally, the complete Bouguer Disturbance δg_B can be calculated as per Equation 3.

Gridding the data using the equivalent sources technique

The equivalent sources technique is a method for interpolating observed potential fields, such as gravimetric and magnetic data. This method involves stipulating a distribution of sources that would produce the observed potential field. The field from these idealized sources can then be calculated anywhere above the measurements. This two-step procedure, an inverse problem followed by a direct calculation, provides a way to continue potential fields from surface to surface (Blakely, 1995). The hypothetical sources must produce a potential field that is harmonic in the area of interest, vanishes at infinity, and reproduces the observed field; they do not need to

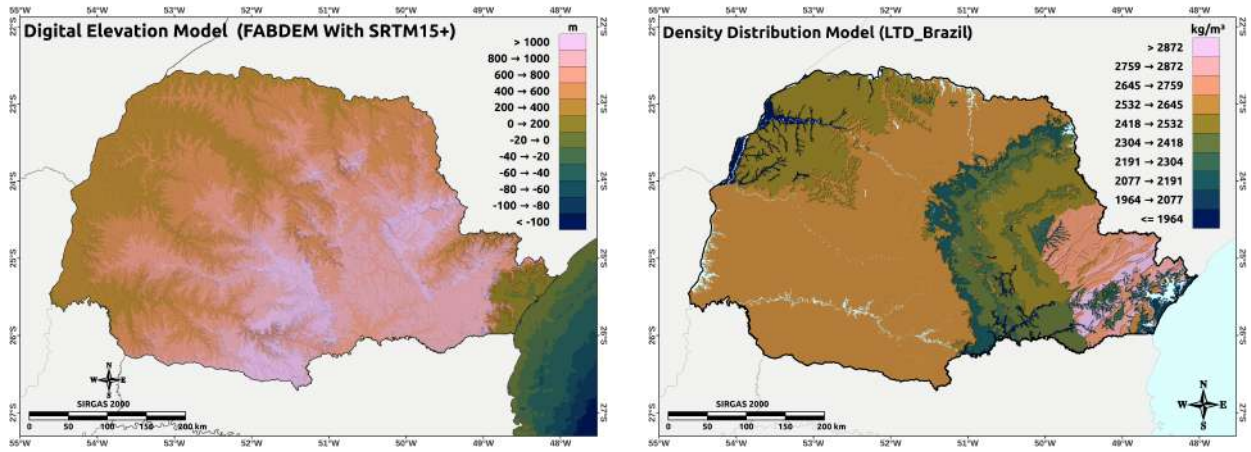

(a) (b)

Figure 5: (a) Digital elevation model, adapted from Tozer et al. (2019) and Hawker et al. (2022); (b) Lateral Topographic Density model for State of Paraná, adapted from de Medeiros et al. (2021).

resemble the true distribution of sources (Blakely, 1995).

Above a plane located below the observation points, it is assumed that there are point sources endowed with the exact properties necessary to simulate a field equivalent to the observed one. That is, the gravitational potential of this idealized arrangement of point sources should be indistinguishable from the potential produced by the actual three-dimensional sources. By defining this equivalent layer, it becomes possible to calculate its potential at any desired point, which, by keeping the depth of this layer within the limits imposed by the data spacing, results in an accurate approximation of the real gravitational field at those same points. Thus, the real field for areas without data can be estimated for interpolation purposes, allowing the projection of a regular grid (Dampney, 1969).

This method is distinguished from conventional techniques (such as weighted average, minimum curvature, or kriging) which interpolate values without considering their specific attributes, as it directly depends on the nature of the data used for interpolation (Cooper, 2000). This ensures the correct analytical behavior of the projected field, providing precision in the interpolation of potential data arranged irregularly and at different elevations (Dampney, 1969; Cooper, 2000).

The ‘EquivalentSources‘ class from the Harmonica library (Fatiando a Terra Project et al., 2023) was used. Three parameters were adjusted for the configuration of the equivalent sources layer: ‘block_size‘, ‘depth‘, and ‘damping‘. The ‘block_size‘ parameter was set to the same value as the grid resolution. ‘Depth‘ was established at 3.5 times the grid resolution value. Finally, a value of 100 was adopted for the ‘damping‘ parameter. The grid was constructed using the ‘verde.grid_coordinates‘ function from the Verde library (Uieda, 2018), which generates coordinates for each point on a regular grid.

The determination of the optimal resolution for gridding the gravimetric data was based on analyzing the distance to the nearest neighbor among the gravimetric stations. Using Python, the distance from each measurement point to its nearest neighbor (nnd) was calculated using the ’CKD-Tree’ data structure (Narasimhulu et al., 2021), and the results were then plotted in the boxplot and histogram (Figure 6).

Based on the analysis of the graphs, the data were divided into three distinct categories: Overlapping Data (nnd $<$ median), Concentrated Data (median $\leq$ nnd $<$ mean), and Scattered Data (nnd $\geq$ mean). It

was observed that the combination of Overlapping and Concentrated Data represented more than 50% of the total data. However, the spatial representativeness of these groups was considered insufficient, as evidenced by their plotting on the map (Figure 7a). In contrast, although the Scattered Data constituted only 27.5% of the total dataset, they demonstrated significantly greater spatial representativeness, as visually verified on the map (Figure 7b). The decision on the gridding resolution was based on the analysis of the distances between the stations of the Scattered Data. A resolution of 1600m was chosen, half the median distance to the nearest neighbor within the Scattered Data, rounded down to the nearest lower multiple of 100.

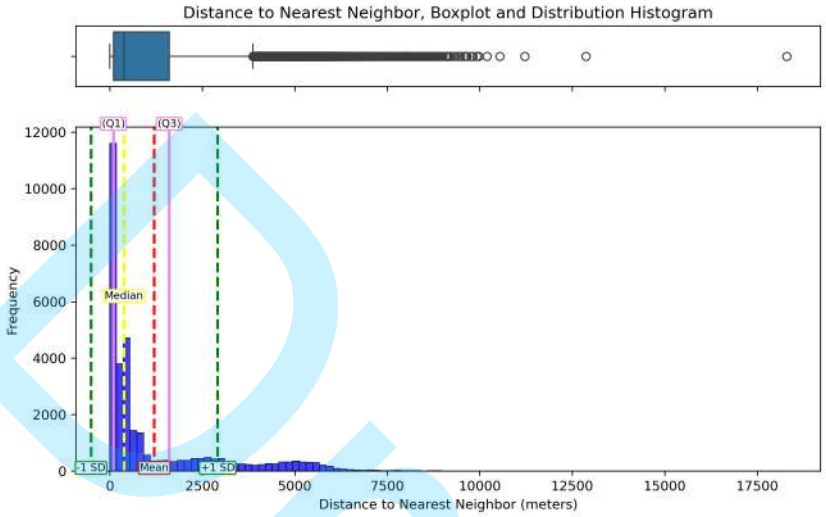

Figure 6: Combined graph illustrating the frequency distribution of the distance to the nearest neighbor. The top part displays a boxplot, detailing the outliers, while the bottom part presents a histogram with indicative lines for the mean (red dashed line), median (yellow dashed line), and the first and third quartiles (yellow dashed lines). The distribution also shows the dispersion in relation to the standard deviation (green dashed lines).

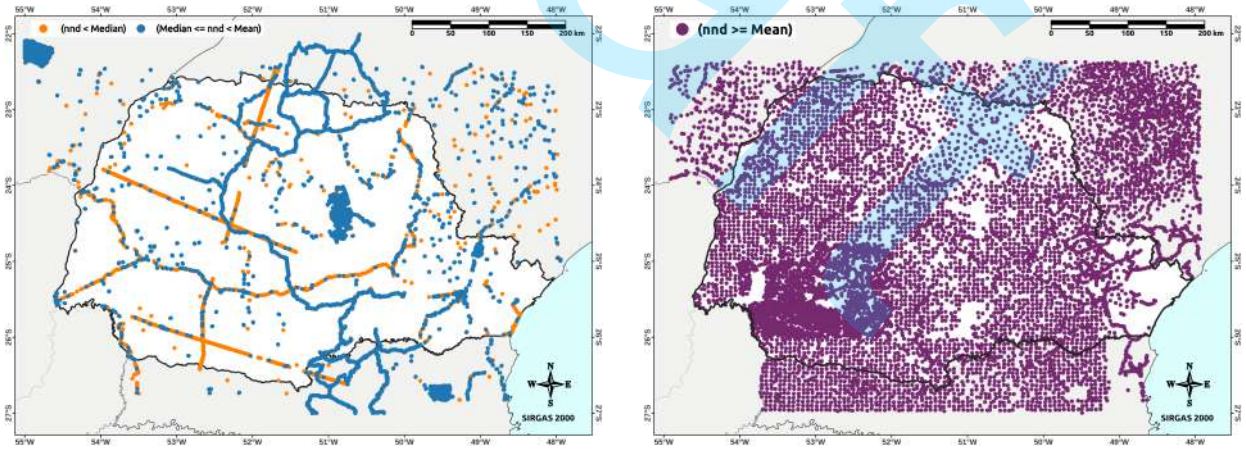

(a) (b)

Figure 7: (a) Overlapping Data (nnd < median) and Concentrated Data (median ≤ nnd < mean); (b) Scattered Data (nnd ≥ mean).

Application of Filters

Data filtering is employed to highlight features in the anomalous gravity field. Predominantly, enhancement filter methods are based on vertical or horizontal derivatives of the gravitational field, or their combinations,

identifying edges or centers of sources through maximum, minimum, or zero values in the transformed data.

The Harmonica library (Fatiando a Terra Project et al., 2023) was used to calculate the horizontal derivatives and the first vertical derivative. The functions harmonica.derivative_easting and harmonica.derivative_northing calculated the horizontal derivatives along the x and y axes, respectively, using the finite difference method, chosen for its accuracy and lack of edge effects.

Horizontal derivatives quantify the rate of change of the potential field in each horizontal direction. If $\phi(x, y)$ represents the field value at a point with coordinates x and y, and Δx and Δy are the uniform sampling intervals in the x and y directions, respectively, the approximate horizontal derivatives at that point can be expressed as (Blakely, 1995):

$$XDR = \frac{\partial \delta}{\partial x} \approx \frac{\delta g_B(x + \Delta x, y) - \delta g_B(x - \Delta x, y)}{2\Delta x}, \tag{4}$$

$$YDR = \frac{\partial \delta}{\partial y} \approx \frac{\delta g_B(x, y + \Delta y) - \delta g_B(x, y - \Delta y)}{2\Delta y}. \tag{5}$$

The first vertical derivative of a potential field is expressed by the limit of the ratio of change of the function ϕ with respect to the variation in the coordinate z, symbolized by Δz, as this variation approaches zero (Blakely, 1995):

$$ZDR = \frac{\partial \delta}{\partial z} = \lim_{\Delta z \to 0} \frac{\delta g_B(x, y, z) - \delta g_B(x, y, z - \Delta z)}{\Delta z}, \tag{6}$$

The Total Horizontal Derivative (THDR) measures the total variation of the potential field on the horizontal surface, regardless of the direction of this variation (Cordell and Grauch, 1985). Its magnitude at a point reflects the intensity of the horizontal variation at that point, which can indicate the proximity of a source edge or an abrupt transition in subsurface properties (Cordell and Grauch, 1985). The THDR is obtained by the square root of the sum of the squares of the horizontal derivatives (Cordell and Grauch, 1985):

$$THDR = \sqrt{\left(\frac{\partial \delta g_B}{\partial x}\right)^2 + \left(\frac{\partial \delta g_B}{\partial y}\right)^2}. \tag{7}$$

Using the relationship between the first vertical derivative and the THDR, the Tilt Derivative (TDR) provides a uniform detection of sources, effectively responding to sources at different depths (Miller and Singh, 1994). The method uses the tilt of the signal to locate sources of potential fields, generating a measure that is positive directly above a source and negative in other regions (Miller and Singh, 1994). The TDR is defined by the inverse tangent of the ratio between the first vertical derivative and the THDR, given by (Miller and Singh, 1994):

$$TDR = \tan^{-1}\left(\frac{\frac{\partial \delta g_B}{\partial z}}{\sqrt{(\frac{\partial \delta g_B}{\partial x})^2 + (\frac{\partial \delta g_B}{\partial y})^2}}\right) = \tan^{-1}\left(\frac{\frac{\partial \delta g_B}{\partial z}}{THDR}\right)$$

Map Layouts

After gridding the data and applying the filters, the Rasterio library (Gillies et al., 2013) was used to convert the results into the GeoTIFF format. The GeoTIFF files were subsequently imported into the QGIS software (QGIS Development Team, 2023), where color scales were set up and layouts were designed.

The cartographic data used originates from the Continuous Cartographic Base of Brazil, at a scale of 1:250,000 (IBGE, 2021). Considering that the State of Paraná spans two zones, UTM 21S and UTM 22S, the SIRGAS 2000 / Brazil Polyconic coordinate reference system was chosen.

To further enhance the anomalies, layers of shaded relief with different vertical exaggerations were overlaid on the maps. The ten colors in the scales divide the values into deciles; the Batlow color scale (Crameri et al., 2020) was chosen for its accuracy in representing data variations in a perceptually uniform manner, without introducing visual distortions. This choice ensures that equivalent increments in the data are perceived as equivalent variations in the visualization (Crameri et al., 2020). The design of this scale takes into account accessibility for individuals with color-related visual impairments, thus expanding data comprehension to a broader audience (Crameri et al., 2020).

RESULTS AND DISCUSSION

Gravity Disturbance in Paraná

Figure 8b illustrates the spatial distribution of the Gravity Disturbance in the study area. At this stage, the effect of the topographic masses has not been accounted for, leading to a strong correlation between the Gravity Disturbance and the topography. For comparison, Figure 8a displays the free-air anomaly as presented in Zanon dos Santos et al. (2022).

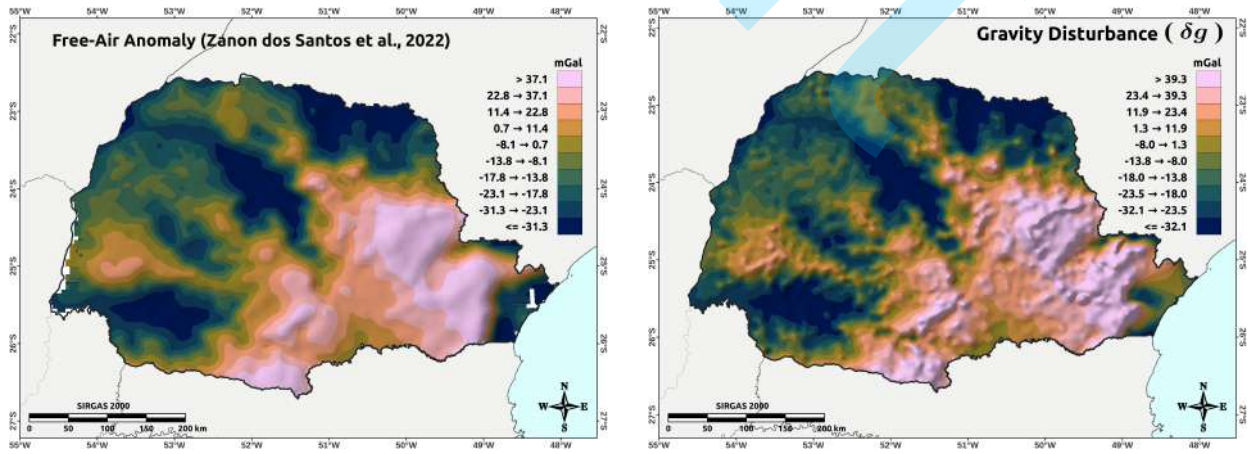

(a) (b)

Figure 8: (a) Free-air gravity anomaly map of the study area by Zanon dos Santos et al. (2022); (b) Gravity Disturbance map of the State of Paraná.

Bouguer Disturbance in Paraná

Figure 9b presents the spatial distribution of the Bouguer Disturbance in Paraná. The Bouguer Reduction involves removing a constant factor from the gravitational effect, equivalent to what would be produced by topographic masses, assuming they had a homogeneous density. As a result, the Bouguer Disturbance reflects the density variations of the topographic masses. For comparison, Figure 9a displays the Bouguer anomaly as presented in Zanon dos Santos et al. (2022).

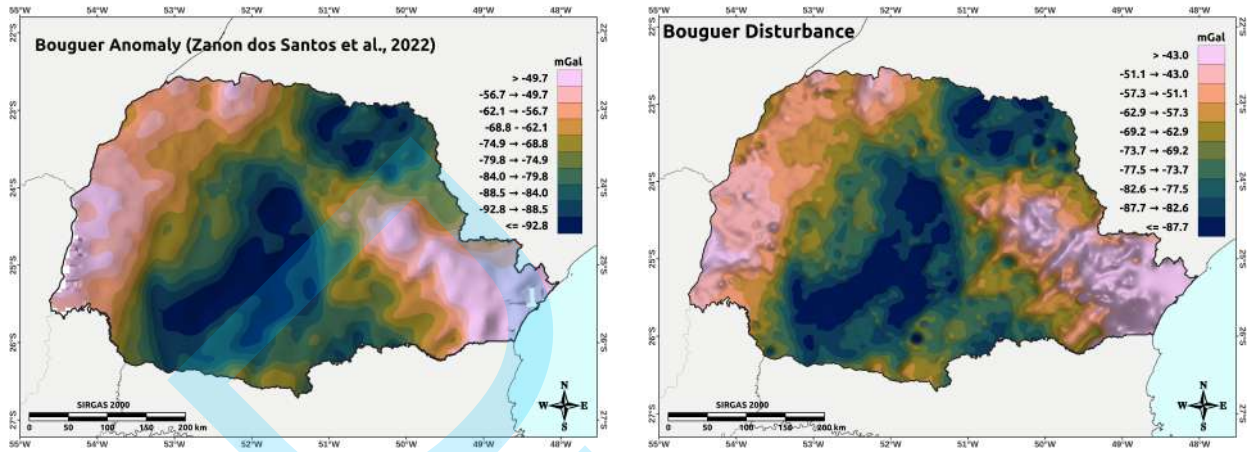

(a) (b)

Figure 9: (a) Bouguer gravity anomaly map of the study area by Zanon dos Santos et al. (2022); (b) Bouguer Disturbance map of the State of Paraná.

In the Bouguer Disturbance (Figure 10), geological features with remarkable gravity response can be separated in two groups, according to their orientations. The first groups is NE-SW oriented, following the orogenic orientation of the Ribeira Belt. Two large amplitude anomalies are in the west-northwest to central area. A remarkable positive anomaly can be noticed in the west-northwest area ($\delta g_B > -60.8\,mGal$), and it matches a classical crustal structure of Paraná Basin basement, the Paranapanema Block, interpreted as a cratonic block (Mantovani et al., 2005). Conversely, deep gravity lows about $\delta g_B < -92.1\,mGal$ are settled in central parts of the state, and most of them worked as basin depocenters, according to previous interpretations (Ferreira et al., 1981; de Souza Filho and Szameitat, 2022). Other areas also were depocenters and have present-day positive gravity response (e.g., NW portion of the Ponta Grossa Arc, (Ferreira et al., 1981; de Souza Filho and Szameitat, 2022)), but they were transformed by posterior magmatic intrusions and crustal bending in the Atlantic opening process. Other NE-SW structures are in the SE portion, clearly related to the Southern Ribeira Belt structures. Some NE-SW linear anomalies are associated with outcropping geological contacts and faulting zones.

The second group of structures is NW-SE oriented, and are closely related to large magmatic intrusions associated with the continental breakup in the South Atlantic (Peate, 1997; Szatmari and Milani, 2016). Dykes, sills and lava flows are part of the significant magmatic activity in this area. However, due to the limitations of the potential field methods in detecting sub-horizontal sheets (Blakely, 1995), lava flows and sills can be hardly detected by gravity, if their borders are not thick enough in relation to the area or the data resolution. On the other hand, the lateral density contrast caused by subvertical sheets generates linear positive anomalies, especially into the sedimentary basin. Therefore, one of the major NW-SE structures in the state is the Ponta

Grossa Dyke Swarm, which crosses the State of Paraná. In between São Jerônimo-Curiúva Lineament (SJCL) and Rio Alonzo fault (RAF) alignments, there are a positive stripe of values in the Bouguer Disturbance ($-92.1\,mGal < \delta g_B < -67.2\,mGal$), contrasting with background values $\delta g_B < -92.1\,mGal$, and corresponds to the principal concentration of vertical sheets in the dyke swarm (Portela Filho and Ferreira, 2003). This structure is even well detailed on magnetic maps, due to the high magnetic susceptibility of these sheets (Ferreira et al., 1981; de Souza Filho and Szameitat, 2022). Stronger than the dyke swarm, is the positive signature of Ponta Grossa Arch ($\delta g_B > -60.8\,mGal$). The complete Ponta Grossa Arch is larger than the studied area (Ferreira, 1982), but the axis of the Ponta Grossa Arch correspond to the area with higher amplitude, in the eastern portion of the state. The NW-SE oriented arch axis partially matches the dyke swarm, but it is limited to about the central State of Paraná, whereas the dyke swarm goes through the Paraná Basin, at least until the Transbrasiliano lineament (de Souza Filho and Szameitat, 2022).

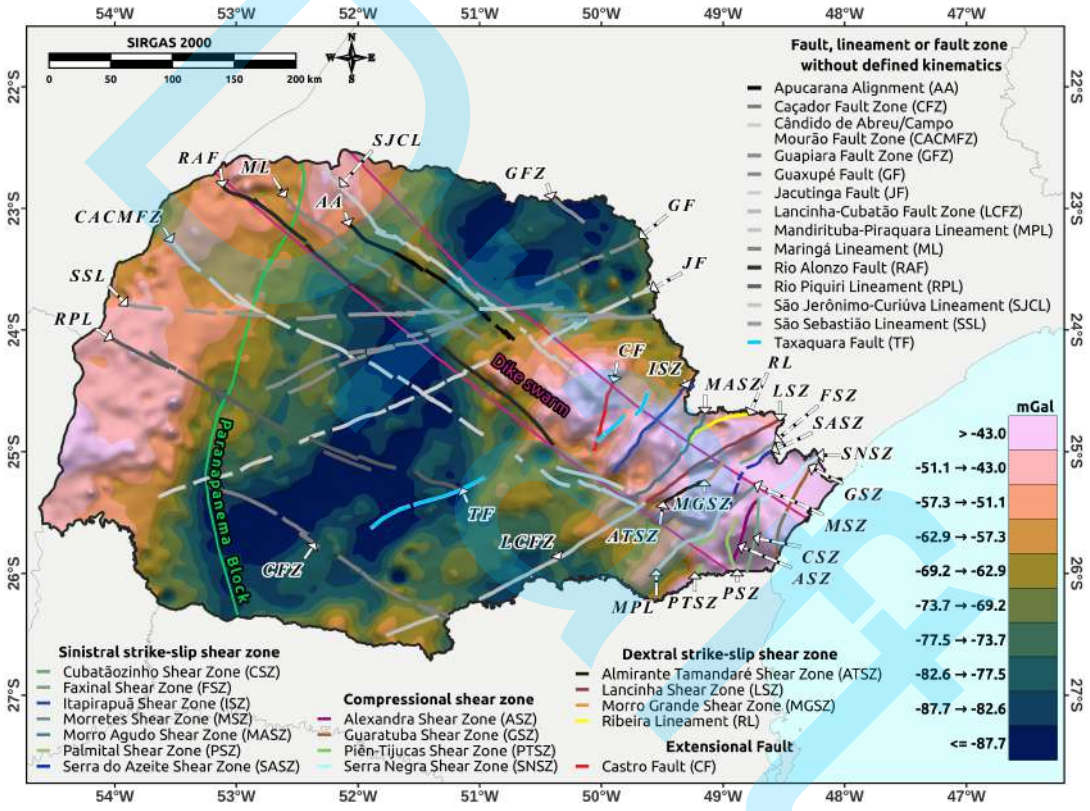

Figure 10: Bouguer Disturbance data in the State of Paraná, overlaid by regional geological features.

Total Horizontal Derivative and Tilt Derivative in Paraná

Figure 11a represents the result of applying the Total Horizontal Derivative (THDR) enhancement filters. The THDR is higher where there are abrupt transitions in the scalar field, such as at contacts among different types of rocks or in fault zones (Cordell and Grauch, 1985). This makes THDR a tool for highlighting geological structures at their edges. Figure 11b represents the result of applying the Tilt Derivative (TDR) enhancement filter. This measure has the unique property of being positive over the source of the anomaly and negative in other areas, which is crucial for identifying the presence and edges of an anomaly (Miller and Singh, 1994). The differential of TDR is its ability to effectively respond to both shallow and deep sources, overcoming limitations

of other techniques that may not clearly identify deeper sources due to lower gradient amplitudes (Miller and Singh, 1994).

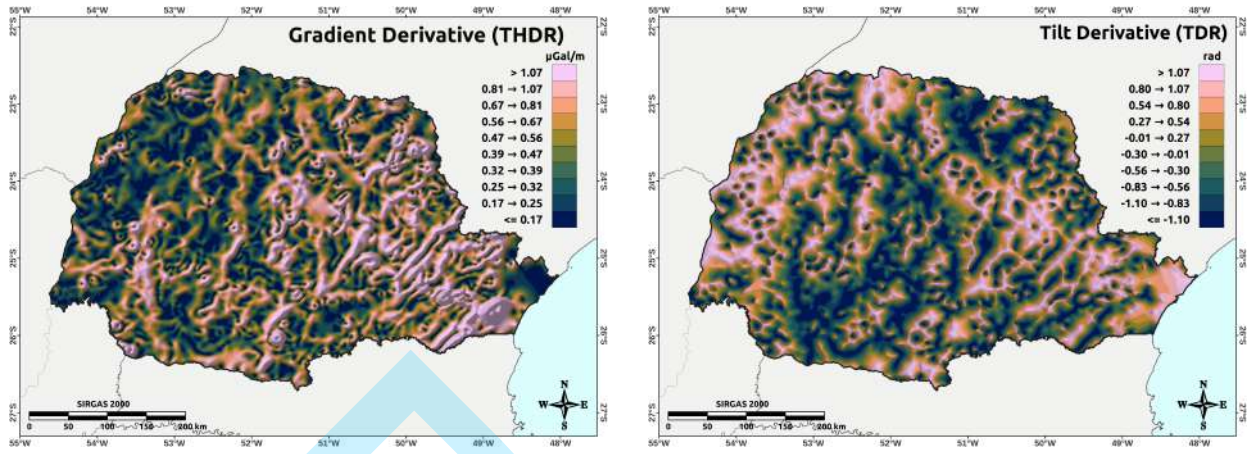

(a) (b)

Figure 11: (a) Total Horizontal Derivative (THDR) map of the gravitational field in the State of Paraná, values in microgals per meter (μGal/m); (b) Tilt Derivative (TDR) map for the State of Paraná, representing the tilt derivative, values in radians.

In the THDR map (Figure 12), it is noticed the detached response of $THDR > 0.66\,\mu$Gal/m, following the RAF structure. Another enhanced structure is the geological contact of the Curitiba Terrane and Luis Alves Terrane, which matches the MPL structure. Southwards, the Rio Piên unit reveals a high amplitude THDR anomaly ($THDR > 1.07\,\mu$Gal/m), possibly given by the lateral density contrast of its high mafic content. Northwards, in the Atuba Complex (Curitiba Terrane), THDR anomalies tend to have lower amplitude, with $THDR < 0.25\,\mu$Gal/m.

The anomalous NW-SE stripe, attributed to the high concentration of sheeted dykes, between SJCL and RAF, was better defined by positive peaks of $TDR > 0.25$ rad (Figure 13). About NE-SW linear features, such as Mandirituba-Piraquara Lineament (MPL), Almirante Tamandaré Shear Zone (ATSZ), Lancinha Shear Zone (LSZ) and Itapirapuã Shear Zone (ISZ), they seem to be better represented by the THDR map.

CONCLUSION

This work compiled a comprehensive dataset of gravimetric data related to the State of Paraná and subjected it to advanced processing techniques, using exclusively open-source tools. The code used in the analysis is available on GitHub, allowing for the replication of results and their use in future research.

We use two alternative techniques for performing the Bouguer calculation and the data gridding. The Gravity Disturbance is our gravity anomaly for the Bouguer calculation, instead of the classical Free-Air Anomaly, in order to avoid inferences in the heights. In the gridding process, we have used the equivalent sources, a suitable method for gravity data with irregular stations distribution.

With the use of the equivalent source interpolation method and the reduction of data by the Gravity Disturbance, the obtained products (Figures 8b, 9b) demonstrate benefits in data analysis for geological interpretations compared to the products generated by Zanon dos Santos et al. (2022) (Figures 8a and 9a).

The resulting Bouguer Anomaly and derived maps have good correlation with first-order gravity structures

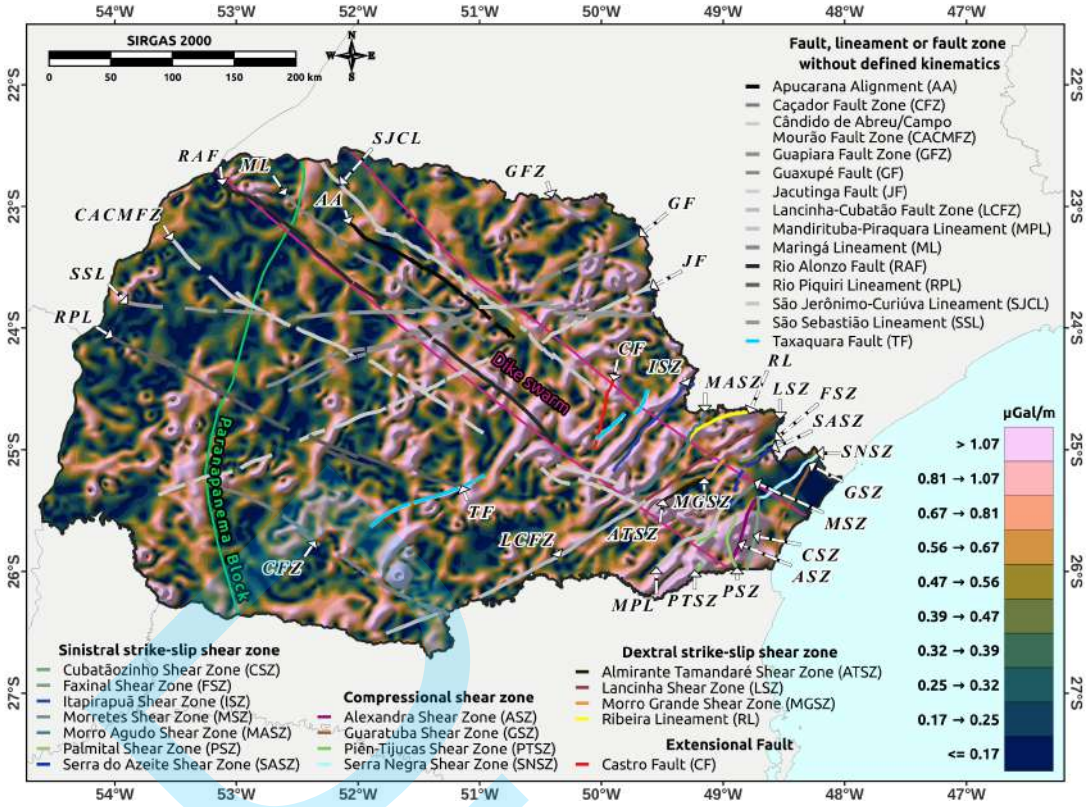

Figure 12: Total Horizontal Derivative (THDR) data of the State of Paraná, overlaid by regional geological features.

in the State of Paraná, corroborating the effectiveness of gravity methods in the detection of contrasting density structures. For example, anomalies higher than -60.8 mGal matched the Paranapanema Block in the western-northwestern portion of the area. Similarly, the outcropping Proterozoic basement encompassed by the Ponta Grossa Arch is one of the most remarkable structures in the Bouguer map.

Beyond the clear contribution to the geophysical characterization of the State of Paraná, this study emphasizes the importance of using advanced geophysical methods in the geophysical investigations, and the benefit of using alternative open-source softwares in the geoscientific analysis.

Finally, the methodology used here represents an alternative mapping approach and a validation option for maps previously created using other methodologies.

ACKNOWLEDGMENTS

We thank the Laboratory of Applied Geophysics Research (LPGA), Federal University of Paraná (UFPR), for the technical support and infrastructure provided for this work. We also thank the Brazilian Federal Agency for Support and Evaluation of Graduate Education (CAPES) for the master's scholarship funding, which enabled the development of this research.

F. J. F. Ferreira was supported in this research by the National Council for Scientific and Technological Development (CNPq – Brazil), under contract 308956/2022-2.

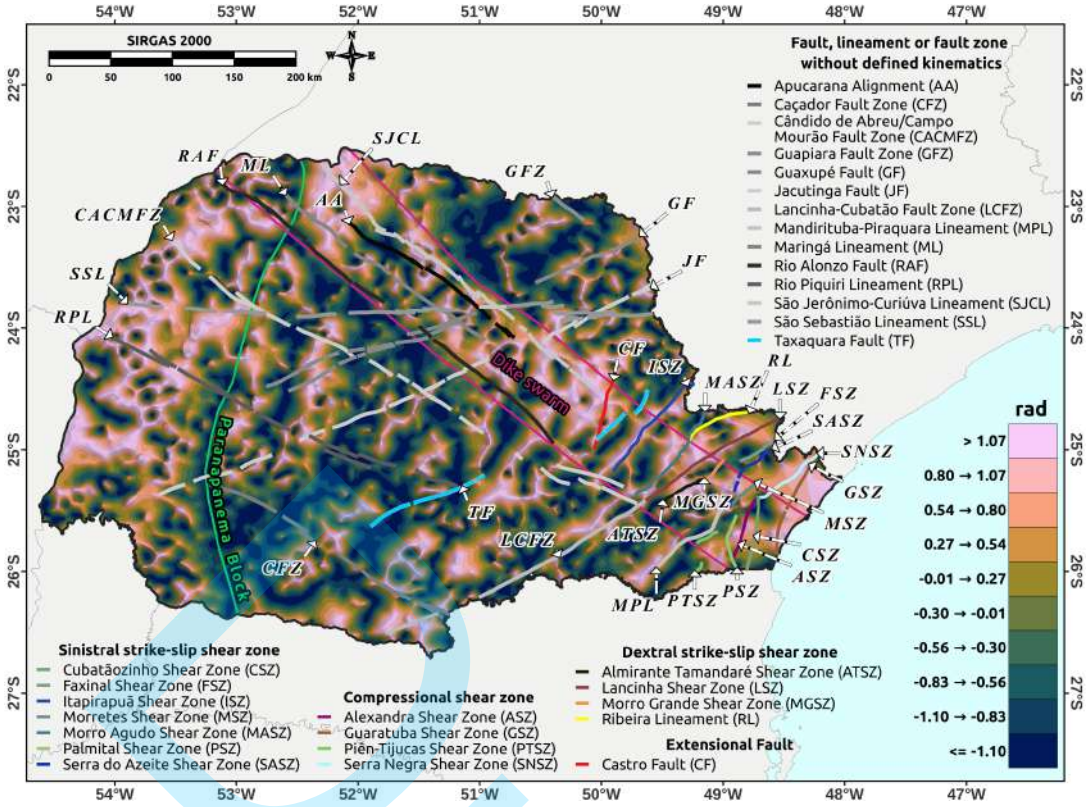

Figure 13: Tilt Derivative (TDR) data of the State of Paraná, overlaid by regional geological features.

DATA AND MATERIALS AVAILABILITY

The data, processing routines, and supporting materials used in this study are publicly available in a GitHub repository at: https://github.com/ErosKerouak/GRAV_PR.git.

REFERENCES

Besser, M. L., M. Brumatti, and A. L. Spisila, 2021, Mapa geológico e de recursos minerais do estado do Paraná. Programa Geologia, Mineração e Transformação Mineral. (1 colored map, 235 x 90 cm, scale 1:600,000).

Blakely, R. J., 1995, Potential theory in gravity and magnetic applications: Cambridge University Press. Cambridge, UK, 464 pp. doi: 10.1017/CBO9780511549816.

Chaves, C., N. Ussami, and J. Ritsema, 2016, Density and P–wave velocity structure beneath the Paraná magmatic province: Refertilization of an ancient lithospheric mantle: Geochemistry, Geophysics, Geosystems, **17**, 3054–3074, doi: 10.1002/2016GC006369.

Cooper, G. R. J., 2000, Gridding gravity data using an equivalent layer: Computers & Geosciences, **26**, 227–233, doi: 10.1016/S0098-3004(99)00089-8.

Cordell, L., and V. J. S. Grauch, 1985, Mapping basement magnetization zones from aeromagnetic data in the San Juan Basin, New Mexico, *in* Hinze, W. J., M. F. Kane, N. W. O'Hara, M. S. Reford, J. Tanner, and C. Weber (Eds.). The Utility of Regional Gravity and Magnetic Anomaly Maps: Society of Exploration Geophysicists, 181–197. doi: 10.1190/1.0931830346.ch16.

Crameri, F., G. E. Shephard, and P. J. Heron, 2020, The misuse of colour in science communication: Nature Communications, **11**, doi: 10.1038/s41467-020-19160-7.

Dampney, C. N. G., 1969, The equivalent source technique: Geophysics, **34**, 39–53, doi: 10.1190/1.1439996.

de Almeida, F. F. M., Y. Hasui, B. B. de Brito Neves, and R. A. Fuck, 1981, Brazilian structural provinces: An introduction: Earth-Science Reviews, **17**, 1–29, doi: 10.1016/0012-8252(81)90003-9.

de Medeiros, D. F., G. Sant'Anna Marotta, E. Yokoyama, I. B. Franz, and R. A. Fuck, 2021, Developing a lateral topographic density model for Brazil: Journal of South American Earth Sciences, **110**, 103425, doi: 10.1016/j.jsames.2021.103425.

de Souza Filho, O. A., and L. S. A. Szameitat, 2022, Contribuição aos estudos geofísicos das Bacias Terrestres Interiores, *in* Souza, M. F. F. d., R. F. Fernandes, and M. F. Alfradique (Eds.). Relatório Subcomitê Potencial de Petróleo e Gás Onshore: Avaliação do potencial de geração de hidrocarbonetos em áreas de bacias sedimentares terrestres: Empresa de Pesquisa Energética (EPE) and Ministério de Minas e Energia (MME), 81–93. url: https://www.epe.gov.br/pt/publicacoes-dados-abertos/publicacoes/reate2020-sct3-avaliacao-do-potencial-de-geracao-de-hidrocarbonetos-em-areas-de-bacias-sedimentares-terrestres.

Fatiando a Terra Project, C. Dinneen, M. Gomez, L. Li, A. Pesce, S. R. Soler, and L. Uieda, 2022, Boule v0.4.1: Reference ellipsoids for geodesy and geophysics. (Software release).

Fatiando a Terra Project, F. D. Esteban, L. Li, V. C. Oliveira Jr., A. Pesce, N. Shea, S. R. Soler, M. Tankersley, and L. Uieda, 2023, Harmonica v0.6.0: Forward modeling, inversion, and processing gravity and magnetic data. (Software release).

Ferreira, F. J. F., 1982, Integração de dados aeromagnéticos e geológicos: configuração e evolução tectônica do Arco de Ponta Grossa: PhD thesis, Universidade de São Paulo (USP), São Paulo, SP, Brasil. (PhD thesis).

Ferreira, F. J. F., R. A. V. Moraes, M. P. Ferrari, and R. B. Vianna, 1981, Contribuição ao estudo do alinhamento estrutural de Guapiara: Proceedings do 3° Simpósio Regional de Geologia, 226–240. Curitiba, PR, Brasil. 226–240.

Gillies, S., et al., 2013, Rasterio: geospatial raster I/O for Python programmers: https://github.com/

rasterio/rasterio. (Open-source geospatial raster processing library).

Götze, H.-J., and X. Li, 1996, Topography and geoid effects on gravity anomalies in mountainous areas as inferred from the gravity field of the central Andes: Physics and Chemistry of the Earth, **21**, 295–297, doi: 10.1016/S0079-1946(97)00051-7.

Harkness, W., 1891, The solar parallax and its related constants: Including the figure and density of the Earth: U.S. Government Printing Office. Washington, D.C., USA, 186 pp. url: https://archive.org/details/solarparallaxits00hark/. (Public domain book).

Hawker, L., P. Uhe, L. Paulo, J. Sosa, J. Savage, C. Sampson, and J. Neal, 2022, A 30 m global map of elevation with forests and buildings removed: Environmental Research Letters, **17**, 024016, doi: 10.1088/1748-9326/ac4d4f.

Heilbron, M., C. M. Valeriano, C. C. G. Tassinari, J. Almeida, M. Tupinambá, O. Siga, and R. Trouw, 2008, Correlation of neoproterozoic terranes between the Ribeira Belt, SE Brazil and its African counterpart: comparative tectonic evolution and open questions: Geological Society, London, Special Publications, **294**, 211–237, doi: 10.1144/sp294.12.

Heiskanen, W. A., and H. Moritz, 1967, Physical geodesy: W. H. Freeman and Company. San Francisco and London, 364 pp.

Hinze, W. J., 2003, Bouguer reduction density: why 2.67?: Geophysics, **68**, 1559–1560, doi: 10.1190/1.1620629.

Hofmann-Wellenhof, B., and H. Moritz, 2006, Physical Geodesy: Springer. Vienna, 403 pp. doi: 10.1007/978-3-211-33545-1.

IBGE, I., 2021, Base Cartográfica Contínua do Brasil, Scale 1:250 000.

Lakshmanan, J., 1991, The generalized gravity anomaly: Endoscopic microgravity: Geophysics, **56**, 712–723, doi: 10.1190/1.1443090.

Li, X., and H.-J. Götze, 2001, Ellipsoid, geoid, gravity, geodesy, and geophysics: Geophysics, **66**, 1660–1668, doi: 10.1190/1.1487109.

Luz, R. T., 2008, Estratégias para modernização da componente vertical do sistema geodésico brasileiro e sua integração ao SIRGAS: Boletim de Ciências Geodésicas.

Mantovani, M. S. M., M. C. L. Quintas, W. Shukowsky, and B. B. Brito Neves, 2005, Delimitation of the Paranapanema Proterozoic block: A geophysical contribution: Episodes, **28**, 18–22, doi: 10.18814/epiiugs/2005/v28i1/002.

Milani, E. J., J. H. G. d. Melo, P. A. d. Souza, L. A. Fernandes, and A. B. França, 2007, Bacia do Paraná: Boletim de Geociências da Petrobras, **15**, 265–287.

Miller, H. G., and V. Singh, 1994, Potential field tilt—a new concept for location of potential field sources: Journal of Applied Geophysics, **32**, 213–217, doi: 10.1016/0926-9851(94)90022-1.

Moritz, H., 1980, Geodetic reference system 1980: Bulletin Géodésique, **54**, 395–405, doi: 10.1007/BF02521480. (IUGG Resolution No. 7; Report of Special Study Group No. 539 of the IAG).

Narasimhulu, Y., A. Suthar, R. Pasunuri, and C. Venkaiah, 2021, CKD-Tree: An improved KD-Tree construction algorithm: Proceedings of the International Semantic Intelligence Conference (ISIC 2021), 211–218. New Delhi, India. 211–218.

Peate, D. W., 1997, The Paraná–Etendeka Province, *in* Mahoney, J. J., and M. F. Coffin (Eds.). Large Igneous

Provinces: Continental, Oceanic, and Planetary Flood Volcanism: American Geophysical Union, **100**, 217–245. doi: 10.1029/GM100P0217.

Portela Filho, C. V., and F. J. F. Ferreira, 2003, Estimativas das taxas de extensão crustal da região central do Arco de Ponta Grossa (Bacia do Paraná) com base em modelagens aeromagnéticas: Presented at the Resumos Expandidos, VIII Congresso Internacional da Sociedade Brasileira de Geofísica, Sociedade Brasileira de Geofísica. Rio de Janeiro, RJ, Brasil.

QGIS Development Team, 2023, QGIS geographic information system: https://www.qgis.org. (Open–source GIS software).

Renne, P. R., M. Ernesto, I. G. Pacca, R. S. Coe, J. M. Glen, M. Prévot, and M. Perrin, 1992, The age of Paraná flood volcanism, rifting of Gondwanaland, and the Jurassic–Cretaceous boundary: Science, **258**, 975–979, doi: 10.1126/science.258.5084.975.

Segawa, J., 1984, Gravity disturbance and the structure of the earth substratum: Zisin (Journal of the Seismological Society of Japan, 2nd ser.), **37**, 621–632, doi: 10.4294/zisin1948.37.4_621.

Siga Júnior, O., 1995, Domínios tectônicos do sudeste do paraná e nordeste de santa catarina: geocronologia e evolução crustal: PhD thesis, Universidade de São Paulo (USP), São Paulo, SP, Brasil.

Soler, S. R., and L. Uieda, 2021, Gradient-boosted equivalent sources: Geophysical Journal International, **227**, 1768–1783, doi: 10.1093/gji/ggab297.

Subiza Piña, H. W., and M. A. d. Sousa, 2001, The gravity database of the Observatório Nacional and the current status of the Brazilian Fundamental Gravity Network: Presented at the 7th International Congress of the Brazilian Geophysical Society, European Association of Geoscientists & Engineers. Salvador, BA, Brazil. doi: 10.3997/2214-4609-pdb.217.327.

Szatmari, P., and E. J. Milani, 2016, Tectonic control of the oil–rich large igneous–carbonate–salt province of the South Atlantic rift: Marine and Petroleum Geology, **77**, 567–596, doi: 10.1016/j.marpetgeo.2016.06.004.

Tozer, B., D. T. Sandwell, W. H. F. Smith, C. Olson, J. R. Beale, and P. Wessel, 2019, Global bathymetry and topography at 15 arc sec: Earth and Space Science, **6**, 1847–1864, doi: 10.1029/2019EA000658.

Turner, S., M. Regelous, S. Kelley, C. Hawkesworth, and M. Mantovani, 1994, Magmatism and continental break-up in the South Atlantic: high precision $^{40}Ar/^{39}Ar$ geochronology: Earth and Planetary Science Letters, **121**, 333–348, doi: 10.1016/0012-821X(94)90076-0.

Uieda, L., 2018, Verde: Processing and gridding spatial data using Green's functions: Journal of Open Source Software, **3**, 957, doi: 10.21105/joss.00957.

Uieda, L., V. Oliveira, and V. Barbosa, 2013, Modeling the Earth with Fatiando a Terra: Proceedings of the 12th Python in Science Conference, SciPy, 92–98. Austin, Texas, USA. 92–98. doi: 10.25080/Majora-8b375195-010.

Zanon dos Santos, R. P., Y. R. Marangoni, C. A. M. Chaves, and G. Sant'Anna Marotta, 2022, New free–air and Bouguer gravity anomaly maps of Brazil: Brazilian Journal of Geophysics, **40**, doi: 10.22564/brjg.v40i6.2195.

Pereira, Eros Kerouak Cordeiro: Conceptualization, Methodology, Software, Data curation, Formal analysis, Visualization, Writing – original draft: **Bongiolo, Alessandra de Barros e Silva:** Supervision, Validation, Writing – review & editing: **Szameitat, Luizemara Soares Alves:** Validation, Investigation, Writing – review & editing: **Rodrigues, Tiago Lima**: Methodology, Validation, Writing – review & editing: **Ferreira, Francisco José Fonseca**: Supervision, Writing – review & editing: